Pergamon

Journal of Structural Geology, Vol. 17, No. 9, pp. 1319 to 1326, 1995

0191-8141/95 $9.50+0.00

0191-8141(95)00033-X

Fault growth by segment linkage: an explanation for scatter in maximum displacement and trace length data from the Canyonlands Grabens of SE Utah

JOSEPH A. CARTWRIGHT, BRUCE D. TRUDGILL* and CHRISTOPHER S. MANSFIELD

Department of Geology, Royal School of Mines, Imperial College of Science, Technology and Medicine, Prince Consort Road, London, SW7 2BP, U.K.

(*Received* 13 *June* 1994; *accepted in revised form* 10 *March* 1995)

Abstract—Maximum displacement (D) and trace length (L) data for a population of 97 normal faults from the Canyonlands Grabens region of SE Utah are presented. Values of L range from 100 to 6500 m, and of D from 1.5–155 m. The data exhibit a scatter between D and L of about half an order-of-magnitude. This is comparable to that exhibited in other published single population datasets. This magnitude of scatter cannot be attributed either to measurement errors or to variation in mechanical properties. We propose that a scatter of this magnitude can be explained by a general model for fault growth by segment linkage, whereby large incremental increases of length attained as fault segments link temporarily exceed incremental increases in displacement. This results in deviations from an idealized growth path, and a step-like evolution expressed between D and L.

INTRODUCTION

Compilations of displacement-length data for faults from a range of tectonic settings have been used to develop general models for fault growth and scaling (Watterson 1986, Walsh & Watterson 1988, Marrett & Allmendinger 1991, Cowie & Scholz 1992a, Gillespie *et al.* 1992). A systematic power-law relationship between maximum displacement (D) and maximum trace length (L) was derived from a compilation of data by Watterson (1986), and was expressed as:

$$D = cL^2 \quad (1)$$

where c is a constant related to a number of material properties, including shear modulus. Recent compilations of D and L data have been used to support or refine the power law growth model proposed by Watterson (Walsh & Watterson 1988, Marrett & Allmendinger 1991, Gillespie *et al.* 1992), or to advocate a linear relationship of the form:

$$D = c^*L \quad (2)$$

where c^* is a critical shear strain (Cowie & Scholz 1992a, b, c, Scholz *et al.* 1993, Dawers *et al.* 1993).

The lack of consensus as to the exact nature of the proposed scaling relationship partly stems from problems associated with compilations of D and L data. One of the most significant problems relates to the large scatter in D against L in most of the data sets (Cowie & Scholz 1992c, Gillespie *et al.* 1992). The scatter in the data is typically an order-of-magnitude in both variables.

The scatter of D–L data has been attributed to: (1) inaccurate data and sampling effects (Walsh & Watterson 1988), (2) variation in material properties (Walsh & Watterson 1988, Cowie & Scholz 1992c), (3) the limitation on accumulation of displacement imposed by isostatic restoring forces (Cowie & Scholz 1992c), and (4) measurement biases (Cowie & Scholz 1992c, Gillespie *et al.* 1992). These measurement biases include the problems of irregular distribution of displacement on the fault surface, the sampling of fault trace length, the complications due to complex fault geometry (splays and segments), and the influence of drag folding.

Several previous publications have suggested that segmented fault geometries may contribute to scatter in D–L data (Peacock & Sanderson 1991, Gillespie *et al.* 1992). However, there has been no detailed analysis of the relative contribution to the total scatter in the D–L characteristics of a single population of faults resulting from segmentation as opposed to the other factors listed above, nor has any specific mechanism been presented to show how the development of segmented geometries can result in a scatter in the data. This lack of quantification of the effect of segmentation on the scatter stems from the rarity of well exposed fault populations with sufficient numbers of faults with sufficient range in D and L to allow statistical analysis.

This paper presents D and L data ranging over three orders of magnitude for 97 normal faults mapped in the Canyonlands Grabens region of SE Utah. The faults all have segmented trace geometries, and the D–L data exhibit a scatter that is comparable to that seen in other single population datasets. The fault system is developed in a layer-cake stratigraphy where significant lateral variations in rock mechanical properties can be disregarded, and where the exposure allows accurate

*Present address: Department of Geological Sciences, University of Colorado at Boulder, Campus Box 250, Boulder, CO 80309-0250, U.S.A.

determinations of tip positions, trace lengths and fault displacement. This means that most of the possible sources of scatter referred to above can be eliminated. An explanation of the scatter in D against L is presented in which it is suggested that growing faults do not rigidly adhere to a given displacement–length scaling law, and a significant component of the total scatter is related to a fundamental growth process whereby faults lengthen by the propagation and linkage of a series of approximately colinear segments. This model of fault growth by segment linkage relates the evolving segmented geometry of a fault to its pathway in a plot of displacement and length. It is concluded that this model can satisfactorily explain the widely observed scatter in D–L data, and the segmented geometry of many types of fault.

THE CANYONLANDS GRABENS

Geological setting

The Canyonlands Grabens have been described by McGill & Stromquist (1975, 1979) and by Trudgill & Cartwright (1994). The Canyonlands Grabens are a gently arcuate system of normal faults covering an area of approximately 2000 km^2, immediately adjacent to the Cataract Canyon of the Colorado River in SE (Fig. 1). All the faults mapped in this region have normal displacements, with maximum displacements of 1–150 m, and trace lengths of 100–6500 m. Most of the faults bound grabens of 200–300 m width (Fig. 1). This structural style is believed to result from gravitational collapse towards the Colorado River induced by the late Pliocene to Pleistocene incision of the Cataract Canyon and the resulting flow of evaporites at depth (Baker 1933, Lewis & Campbell 1965, McGill & Stromquist 1975, 1979, Huntoon 1982, Trudgill & Cartwright 1994).

The stratigraphy consists of a brittle upper layer approximately 500 m thick, which is composed mainly of Pennsylvanian to Early Permian sandstones and limestones, overlying a ductile layer consisting of a mixed carbonate and evaporite sequence more than 300 m thick (the Paradox Member) (Fig. 2).

Exhumation joints are pervasively developed in the sandstones and limestones. They pre-date the collapse faulting and influenced the detailed geometry of the graben-bounding faults (McGill & Stromquist 1979, Trudgill & Cartwright 1994). Variability in the joint set distributions in the Canyonlands area is believed to represent the only major variation in the mechanical properties of the deformed brittle sequence (Trudgill & Cartwright 1994).

Cross-sectional geometry

The cross-sectional geometry of the faults is constrained down to the top of the evaporite sequence in a series of tributary canyons to the Colorado River (e.g. Cross Canyon, Lower Red Lake Canyon, Fig. 1). Traverses along three of the tributary canyons are summarized in the diagrammatic cross-section in Fig. 2. The graben-bounding faults are vertical at surface, and remain vertical to sub-vertical for the 400–500 m distance to the top of the evaporite sequence (cf. Trudgill & Cartwright 1994, fig. 3). No evidence was found in these traverses for structural intersection between pairs of graben-bounding faults at depth as previously suggested by McGill & Stromquist (1979) and Trudgill & Cartwright (1994).

Stratigraphic correlations show that fault displacement is constant from the surface down to levels close to the top of the evaporites. This indicates that fault displacement measured at the surface can be assumed to represent the maximum value for that part of a fault. At depth, fault planes are recognizable as zones typically 1–3 m wide, consisting of fault gouge and fault breccia. These fault zones open upwards into fissures several metres wide within the top 200 m of the surface (Biggar *et al.* 1981), and are filled partly or wholly with rubble and aeolian sediment (Fig. 2). This suggests that the fault planes must have been open as tensile fissures to depths approaching half the thickness of the brittle sedimentary succession, and that the earliest propagation of the graben-bounding faults was a tensile opening with a downward directed propagation. This interpretation contrasts with the upward propagation model of McGill & Stromquist (1979).

Map-view geometry and segmentation

The faults mapped in the Canyonlands are all segmented in plan view: i.e. they are composed of a number of discrete segments. Trudgill & Cartwright (1994) showed that segment boundaries consist of relay structures that exhibit a range of structural styles that are broadly comparable with the evolutionary scheme proposed by Peacock & Sanderson (1991). In this scheme, relay structures proceed from a stage where fault segments overlap with an intervening relay ramp, to a more evolved stage where the relay ramp has broken down by internal faulting and a through-going fault zone connects the overlapping segments. Trudgill & Cartwright (1994) identified several 'orders' of segmentation corresponding to order-of-magnitude variation in typical length scales of individual segments. They proposed that the different scales of segmentation were related to different forms of mechanical anisotropy, including the influence of basement structure at depth, brittle layer thickness, and joint length and spacing.

FAULT PARAMETERS

All the faults in the mapped area with isolated tips at both ends of the fault trace, and whose tips could be mapped accurately were included in the fault database. The latter condition introduces a lower limit for faults with a maximum displacement of about 1.5 m, and about 100 m trace length. Out of a total of over 140 faults mapped, 97 satisfy these criteria for inclusion in the

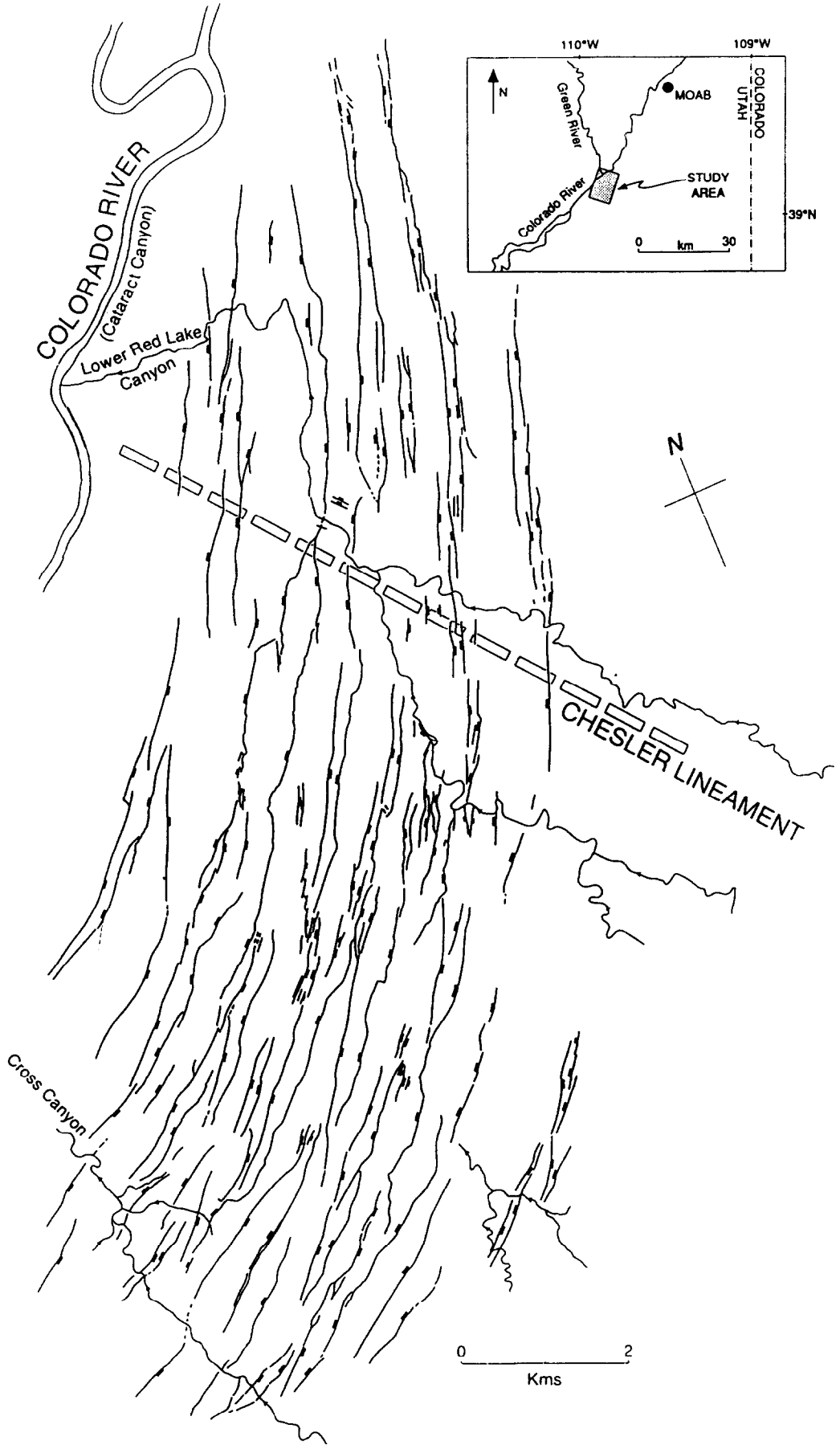

Fig. 1. Fault map of northern sector of the Canyonlands Grabens area, western U.S.A. Over 140 faults have been mapped in this region, but only 97 are included in the database of displacement and length values, most of which are included on this map. Solid ticks indicate the downthrown side of a normal fault. The location of the study area is shown in the small inset map of SE Utah.

analysis. We treat segmented faults as single faults for the purposes of *D–L* analysis, and measure trace lengths from tip to tip of the external segments.

Measurement of D *and* L

Lateral tips were located initially using USGS 1:33,000 aerial photographs, with 1:5,000 mapping being undertaken in the field to locate their position accurately. The resolution of enlarged aerial photographs is 1–2 m, and tips can usually be located to within 10–20 m. The maximum error in any of the trace length measurements is estimated at no more than 5%, with most of the values incorporating errors of less than 2%.

Throw was measured by surveying the elevation difference between equivalent strata exposed at the footwall crest and at the hangingwall cut-off. Since the drop of the fault planes exposed at surface is always within a few degrees of vertical, the throw is a close approximation to the displacement. The full exposure of footwall bedding on the fault planes allows displacement variations along faults to be analysed, and is a valuable constraint for the location of the position of maximum displacement.

Where the hangingwall strata are covered by sediments, the throw was estimated using an estimate of the cover thickness, often measured in stream sections, swallow holes and fissures. Measured thicknesses ranged from 0.5 to 12 m, with the majority of values ranging from 3–7 m. The maximum error (surveying error plus error in cover thickness) in fault displacements is less than 10%.

Results

The *D* vs *L* data for the 97 faults surveyed are shown in Fig. 3. The range of both *D* and *L* is approximately three orders-of-magnitude, which should be sufficient to define a scaling relationship, if such a relationship is applicable. When plotted on normal axes (Fig. 3a), the data exhibit a pronounced scatter of about half an order-of-magnitude in both variables. The extent of this scatter is too large to justify regressing the data (Gillespie *et al.* 1992), and only the most general trend towards increasing values of *D* with *L* can be deduced from the data. On log–log axes (Fig. 3b), the data cluster in a broad band with a linear trend. Faults with trace lengths greater than about 250 m lie within the field of multi-population data compiled by Gillespie *et al.* (1992), the outline of which is shown in Fig. 3(b).

The larger scatter in the multi-population compilation dataset is partly the result of combining data from different sources (Cowie & Scholz 1992c).

The scatter in the Canyonlands data is comparable to that exhibited by single population datasets reviewed by Cowie & Scholz (1992c). Whilst it is possible that a significant proportion of the scatter in previously compiled datasets is due to measurement error (Gillespie *et al.* 1992), only a small component (<10%) of the scatter in the Canyonlands dataset can be attributed to measurement errors (Fig. 3b). Since the majority of the Canyonlands faults plot within the field of data compiled by Gillespie *et al.* (1992), this suggests that valid comparisons can be made between the various datasets, and also that any explanation for the scatter in the Canyon-

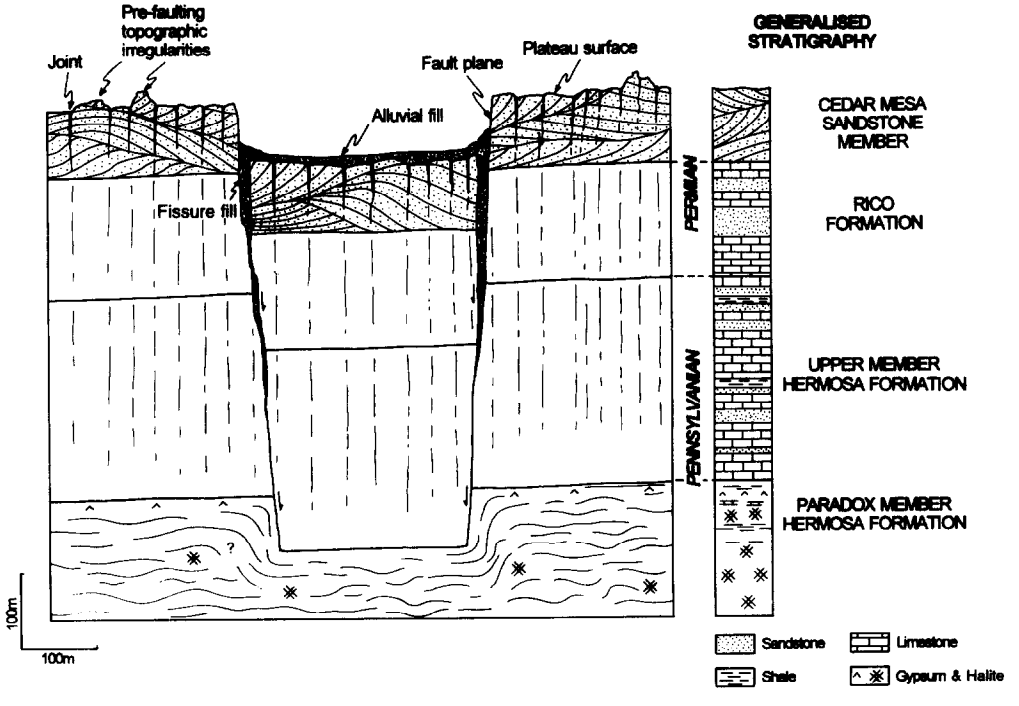

Fig. 2. Generalized cross-section across a graben in the Canyonlands based on traverses of several tributary canyons to the Cataract Canyon (e.g. Lower Red Lake Canyon, Cross Canyon, shown on Fig. 1).

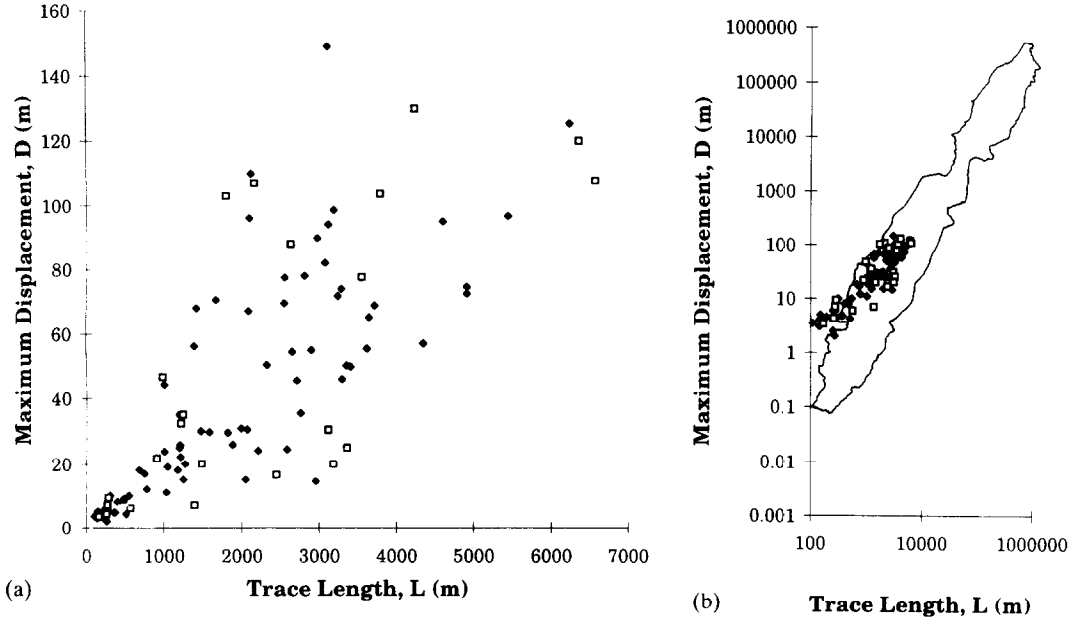

Fig. 3. Maximum displacement (D) vs trace length (L) data for 97 faults surveyed in the Canyonlands Grabens, on (a) normal scale axes and (b) log–log axes, showing a general trend towards increasing D with L, but with a large scatter (approximately five-fold) in both variables. All of these faults are segmented, but the data shown here refer to the values for the whole fault in each case, not the component segments comprising individual faults. Errors in the values are less than 10%. The outline of a compilation of D–L data presented by Gillespie *et al.* (1992) is shown in (b), and confirms that most of the faults in the Canyonlands lie within the general field of fault data, and have a similar scatter in D and L. The square symbols refer to faults from the sub-area northeast of the Chesler Lineament (see Fig. 1), where the surface rocks are marked by two penetrative joint sets. The diamonds refer to faults from the sub-area southwest of the Chesler Lineament, where the joints are less pronounced. The scatter exhibited by these two sub-sets is similar, and suggests that the difference in mechanical properties related to different jointing characteristics of the two areas was not influential in producing the scatter in the data.

lands data may have a bearing on the scatter in other datasets.

DISCUSSION

The Canyonlands provides an ideal area for a compilation of single population D–L dataset for use in evaluating models of fault growth and fault scaling relationships. The data on 97 faults presented here is the largest compilation so far achieved from a single area over which the mechanical and lithological boundary conditions are relatively uniform. The only other area with comparable size range and exposure of faults in one tectono-stratigraphic province is the Volcanic Tablelands of Eastern California (Dawers *et al.* 1993), but the number of faults in this dataset amounts to only 15, and their cross-sectional geometry is poorly constrained.

One possible limitation with the faults in the Canyonlands is that they root at depth into ductile structures whose geometry is poorly constrained (Fig. 2). This brittle–ductile deformation style could mean that the D–L data cannot be compared in an absolute sense with those derived from truly brittle, isolated, blind faults (Gillespie *et al.* 1992). The D–L data for the Canyonlands (Fig. 3b) plot generally within the field of D–L values compiled by Cowie & Scholz (1992c) and Gillespie *et al.* (1992), however, so we consider a qualitative comparison between these datasets to be valid.

Figure 3 shows a large degree of scatter in D with L. Of the explanations for the scatter referred to in the introduction (measurement error, sampling, variation in material properties, isostatic limitations, and measurement biases from a segmented geometry) only the influence of segmentation is considered to be capable of accounting for the scatter in the Canyonlands data. Explanations based on measurement error can be eliminated simply by comparing the five-fold scatter in the data with the maximum errors in measurement of D and L of 10%. Sampling of maximum trace length and displacement is not considered a problem since the cross-sectional traverses show that displacement is a maximum at the surface.

Variation of mechanical properties in the deforming rock units is potentially a more probable source of a significant proportion of the scatter in the Canyonlands data. These variations could conceivably be related to lithological variations, or to variations in the joint systems. Lateral variations in lithology in the Canyonlands Grabens are restricted to minor facies variations on a scale of 10–100 m (Lewis & Campbell 1965). Such lithological variation is therefore unlikely to have influenced mechanical properties on the length scale of faults in the area. McGill & Stromquist (1979) and Trudgill & Cartwright (1994) document a change in joint style across the Chesler Lineament (Fig. 1), but since there is no obvious difference in the degree of scatter in the D–L data for faults from the two areas (Fig. 3), it is concluded that the joint characteristics, and hence any material properties related to joint style, are not a significant factor contributing to the scatter in the D–L data.

Fault growth by segment linkage as an explanation of the scatter in D–L *data*

Current models providing a conceptual framework to explain the processes involved in fault growth fall into two broad groups, (1) growth by radial propagation (Watterson 1986, Walsh & Watterson 1988, Cowie & Scholz 1992a,b), and (2) growth by segment linkage (Segall & Pollard 1980, Segall 1984, Pollard & Aydin 1984, Granier 1985, Gudmundsson 1987, Martel *et al.* 1988, Peacock & Sanderson 1991, Dawers *et al.* 1993, Gawthorpe & Hurst 1993, Anders & Schlische 1994, Jackson & Leeder 1994, Trudgill & Cartwright 1994).

The contrast between these two types of fault growth model is illustrated in Fig. 4. A fault growing by radial propagation (Fig. 4a) follows a growth path that is prescribed by a scaling or growth law of the type shown in equations (1) and (2). Provided that the material properties are constant throughout the period of the deformation, incremental increases in D and L are such that the fault remains on this linear growth path (in a log D vs log L plot) throughout its evolution.

In contrast, in the model of fault growth by segment linkage, growth consists of the propagation, interaction and linkage of segments. A fault growing in this way would follow a complex, step-like growth path (Fig. 4b). In the initial stage, several fault segments are shown growing towards each other by radial propagation (Fig. 4b, stage i). Each segment could be compared at this stage with the pathway followed by the fault shown in Fig. 4(a), i.e. increases in D and L would be related by the appropriate growth law for this specific deformational context. As overlap occurs, stress fields in the tip regions are altered (Segall & Pollard 1989), further propagation tends to be inhibited, and D/L ratios for individual segments will tend to increase (Peacock & Sanderson 1991). The path followed by both individual segments and the segmented fault zone will in this case both deviate from the growth line for radial propagation (Fig. 4b, stage ii). Individual segments with increased D/L ratios will deviate above the line, whereas the newly linked segmented fault will deviate beneath the growth line simply because of the disproportionate increase in length achieved during segment linkage (Scholz *et al.*

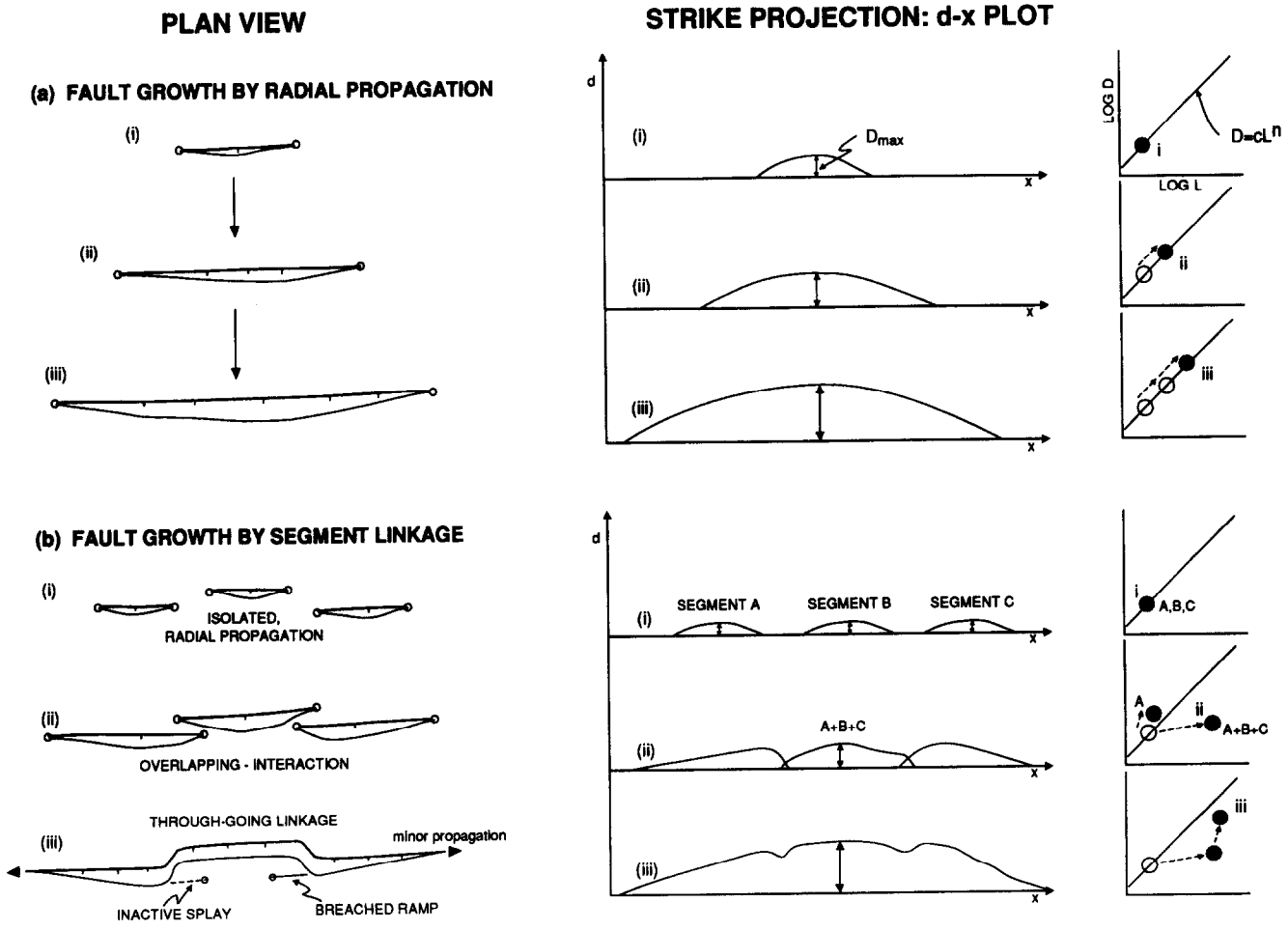

Fig. 4. A comparison of two models of fault growth (a) radial propagation, and (b) segment linkage. Three stages of growth are compared for both models in plan view, on a displacement (d) against distance (x) plot, and on a log maximum displacement (D) vs log trace length (L) plot. The most important difference is seen on the contrasting pathways followed on the log D–log L plots, with the radially propagating fault following a linear and predictable growth path, but the segmented fault following a step-like and unpredictable path. Note that individual segments may deviate above an idealized gowth line as they begin to interact with neighbouring segments [A in stage ii, shown on the log–log plot in (b)], but the newly segmented fault as a whole will deviate beneath this idealized line, since the sum of the lengths of the individual segments comprising the segmented fault will produce a much longer trace length for only limited increase in maximum displacement.

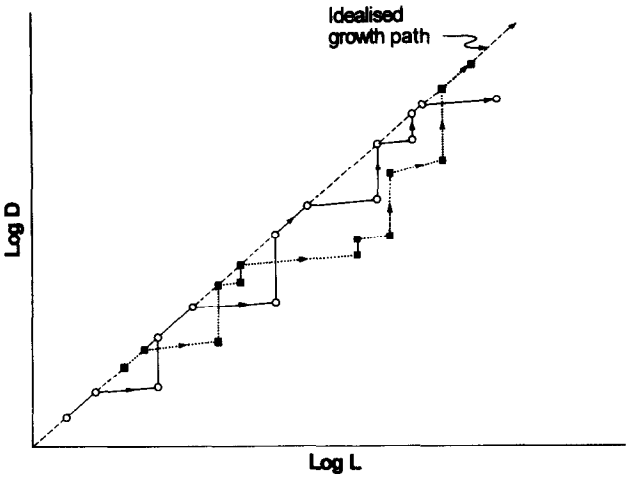

Fig. 5. Hypothetical pathways on a plot of log maximum displacement (D) vs log trace length (L) taken by two faults growing by several cycles of segment linkage. Each cycle of segment linkage is marked by a departure from an idealized linear growth path. The size of the 'steps' would depend on the lengths and numbers of segments involved in each cycle of linkage. The D–L values of a population of faults growing by segment linkage would exhibit a scatter that is represented schematically by these 'step-like' growth paths.

1993). The final stage in the growth cycle is marked by accumulation of displacement on the linked fault with little or no radial propagation and increase in length. By increasing D for relatively minor increase in L, the fault would follow a path taking it back towards the growth line (Fig. 4b, stage iii). Once a critical D/L ratio was re-established, radial propagation could proceed as for stage (i) until further interactions with neighbouring structures led to a repeat of this step-like departure from the growth line. Repetition of this three-stage cycle would lead to a fault comprising a hierarchy of segments with different length scales, as is observed for all the faults mapped in the Canyonlands (Trudgill & Cartwright 1994).

How does this model of fault growth by segment linkage explain the scatter in the D–L data for the Canyonlands? At any instant in the evolution of a fault population within a specific tectonic province, individual faults growing according to this model would be at different stages on their own particular step-wise growth curve (Fig. 5). Some would be in a stage of radial propagation following a path along the growth line appropriate for the mechanical boundary conditions. Others would be at different stages of overlap, interaction and linkage, probably with different length scales and numbers of segments involved. These faults would have D and L values lying beneath the growth line, with growth paths and positions reflecting their own specific histories of linkage. The variability in the timing and length scale of linkage to be expected in any natural fault system would produce a scatter in the D–L data. The magnitude of the scatter would be largely a function of the numbers and lengths of segment involved during a typical cycle of linkage. Faults in the Canyonlands often consist of more than 10 primary segments of broadly similar length, and these in turn all consist of several secondary segments (Trudgill & Cartwright 1994). If linkage of most of these primary segments occurred over a relatively short time interval in which there was only minor addition of displacement, then this would easily account for the five-fold scatter in D with L (Fig. 3).

The model of growth by segment linkage illustrated in Fig. 4(b) thus offers a simple explanation for both the observed scatter of D–L data from the Canyonlands fault population, and the range of morphological characteristics of segmented faults and segment boundaries (Trudgill & Cartwright 1994). Given the similarity in the degree of scatter in the fault data from the Canyonlands with other single population datasets (Cowie & Scholz 1992c, Gillespie *et al.* 1992), then it is suggested that a significant component of the scatter recorded in these other datasets could also be explained by the process of segment linkage.

CONCLUSIONS

(1) D and L data compiled for 97 faults from the Canyonlands Grabens area of SE Utah exhibit a crude scaling between D and L over a range of about three orders-of-magnitude in both variables. The scatter in the data is about half an order-of-magnitude in both variables.

(2) Measurement error, sampling problems, and variations in the mechanical properties of the rock units do not cause significant scatter in the data.

(3) The scatter in the Canyonlands data can be explained by a model of fault growth by segment linkage, in which the growth path plotted for D and L is step-like, corresponding to linkage cycles.

Acknowledgements—Fina Exploration Ltd (JAC and BDT), the Nuffield Foundation (JAC), and Shell U.K. Ltd are thanked for their financial assistance. John Walsh, David Peacock, Patience Cowie, Raymond Franssen, John Cosgrove and Anabel Macleod are thanked for reviewing the manuscript. Faisal Jaffri and Simon Harper are thanked for assistance in the field. The kind assistance of the National Park Service staff at the Needles District Ranger Station and in the district office in Moab are gratefully acknowledged.

REFERENCES

Anders, M. H. & Schlische, R. W. 1994. Overlapping faults, intrabasin highs, and the growth of normal faults. *J. Geol.* **102**, 165–180.

Baker, A. A. 1933. Geology and oil possibilities of the Moab district, Grand and San Juan counties, Utah. *U.S. geol. Surv. Bull.* **841**.

Biggar, N. E., Harden, D. R. & Gillam, M. L. 1981. Quaternary deposits in the Paradox Basin. *Rocky Mountain Assoc. Geol.*, 1981 Field Conference, 129–137.

Cowie, P. A. & Scholz, C. H. 1992a. Physical explanation for the displacement–length relationship of faults using a post-yield fracture mechanics model. *J. Struct. Geol.* **14**, 1133–1148.

Cowie, P. A. & Scholz, C. H. 1992b. Growth of faults by accumulation of seismic slip. *J. geophys. Res.* **97**, 11,085–11,095.

Cowie, P. A. & Scholz, C. H. 1992c. Displacement–length scaling relationship for faults: data synthesis and discussion. *J. Struct. Geol.* **14**, 1149–1156.

Dawers, N. H., Anders, M. H. & Scholz, C. H. 1993. Growth of normal faults: displacement–length scaling. *Geology* **21**, 1107–1110.

Gawthorpe, R. L. & Hurst, J. M. 1993. Transfer zones in extensional

basins: their structural style and influence on drainage development and stratigraphy. *J. geol. Soc. Lond.* **150**, 1137–1152.

Gillespie, P. A., Walsh, J. J. & Watterson, J. 1992. Limitations of dimension and displacement data from single faults and the consequences for data analysis and interpretation. *J. Struct. Geol.* **14**, 1157–1172.

Granier, T. 1985. Origin, damping and pattern of development of faults in granite. *Tectonics* **4**, 721–737.

Gudmundsson, 1987. Geometry, formation and development of tectonic fractures on the Reykjanes Peninsular, southwest Iceland. *Tectonophysics* **139**, 295–308.

Huntoon, P. W. 1982. The Meander anticline, Canyonlands, Utah: An unloading structure resulting from horizontal gliding on salt. *Bull. geol. Soc. Am.* **93**, 941–950.

Jackson, J. & Leeder, M. 1994. Drainage systems and the development of normal faults: an example from Pleasant Valley, Nevada. *J. Struct. Geol.* **16**, 1041–1059.

Lewis, R. Q., Sr. & Campbell, R. H. 1965. Geology and uranium deposits of Elk Ridge and vicinity, San Juan County, Utah. *Prof. Pap. U.S. geol. Survey*, **351**.

Machette, M. N., Personius, S. F., Nelson, A. R., Schwartz, D. P. & Lund, W. R. 1991. The Wasatch fault zone, Utah: segmentation and history of Holocene earthquakes. *J. Struct. Geol.* **13**, 137–149.

Marrett, R. & Allmendinger, R. W. 1991. Estimates of strain due to brittle faulting: sampling of fault populations. *J. Struct. Geol.* **13**, 735–737.

Martel, S. J., Pollard, D. D. & Segall, P. 1988. Development of simple strike-slip fault zones, Mount Abott Quadrangle, Sierra Nevada, California. *Bull. geol. Soc. Am.* **100**, 1451–1465.

McGill, G. E. & Stromquist, A. W. 1975. Origin of graben in the Needles District, Canyonlands National Park, Utah. *Four Corners geol. Soc. Guidebook, 8th Field Conference, Canyonlands*, 235–243.

McGill, G. E. & Stromquist, A. W. 1979. The grabens of Canyonlands National Park, Utah: geometry, mechanics and kinematics. *J. geophys. Res.* **84**, 4547–4563.

Peacock, D. C. P. & Sanderson, D. J. 1991. Displacements, segment linkage and relay ramps in normal fault zones. *J. Struct. Geol.* **13**, 721–733.

Pollard, D. D. & Aydin, A. 1984. Propagation and linkage of oceanic ridge segments. *J. geophys. Res.* **89**, 10,017–10,028.

Scholz, C. H., Dawers, N. H., Yu, J.-Z., Anders, M. H. & Cowie, P. A. 1993. Fault growth and fault scaling laws: preliminary results. *J. geophys. Res.* **98**, 21,951–21,961.

Segall, P. 1984. Formation and growth of extensional fracture sets. *Bull. geol. Soc. Am.* **95**, 454–462.

Segall, P. & Pollard, D. D. 1980. Mechanics of discontinuous faults. *J. geophys. Res.* **85**, 4337–4350.

Trudgill, B. D. & Cartwright, J. A. 1994. Relay ramp forms and normal fault linkages—Canyonlands National Park, Utah. *Bull. geol. Soc. Am.* **106**, 1143–1157.

Walsh, J. J. & Watterson, J. 1987. Distributions of cumulative displacement and seismic slip on a single normal fault surface. *J. Struct. Geol.* **9**, 1039–1046.

Walsh, J. J. & Watterson, J. 1988. Analysis of the relationship between displacement and dimensions of faults. *J. Struct. Geol.* **10**, 239–247.

Walsh, J. J. & Watterson, J. 1990. New methods of fault projection for coalmine planning. *Proc. Yorks. geol. Soc.* **48**, 209–219.

Walsh, J. J. & Watterson, J. 1991. Geometric and kinematic coherence and scale effects in normal fault systems. In: *The Geometry of Normal Faults* (edited by Roberts, A. M., Yielding, G. & Freeman, B.). *Spec. Publ. geol. Soc. Lond.* **56**, 193–206.

Watterson, J. 1986. Fault dimensions, displacements and growth. *Pure & Appl. Geophys.* **124**, 365–363.